Extended Abstracts of the 1997 International Conference on Solid State Devices and Materials, Hamamatsu, 1997, pp. 40-41

Fine-Grained $SrBi_2Ta_2O_9$ Thin Films by Low Temperature Annealing

Nobuhito OGATA, Yasuyuki ITO, Kazuya ISHIHARA, Masaya NAGATA, Hitoshi URASHIMA, Akira OKUTOH, Shinobu YAMAZAKI, Shun MITARAI, and Jun KUDO

Functional Devices Laboratories, Sharp Corporation, 2613-1 Ichinomoto-cho, Tenri-shi, Nara 632, Japan

Phone: +81-7436-5-3489, Fax: +81-7436-5-2774, E-mail: ogata@icg.sharp.co.jp

1. Introduction

$SrBi_2Ta_2O_9$(SBT) is one of the most attractive materials for the ferroelectric nonvolatile memory application, since it has fatigue-free properties and small coercive field (Ec) than $Pb(Zr,Ti)O_3$[1]-[5]. However, SBT needs high crystallization temperature of around 800℃ in oxgen ambient, which results in a serious damage to the stacked cell structure required for the highly integrated ferroelectric memories. Further, as a result, a porous, large-grained structure causes the low breakdown voltage and the difficulty of precise petterning of the ferroelectric capacitor.

In this paper, we propose the new metalorganic decomposition (MOD) processing using low pressure[6] and low temperature annealing to improve the film quality. Surface morphologies, cross-sectional structures, and electrical properties of SBT films were investigated.

2. Experimental

SBT thin films were prepared on Pt(100nm)/TiO_2 (40nm)/SiO_2(600nm)/Si substrates by the MOD method. The molar ratio of Sr/Bi/Ta in the MOD solution was 1.0/2.2/2.0.

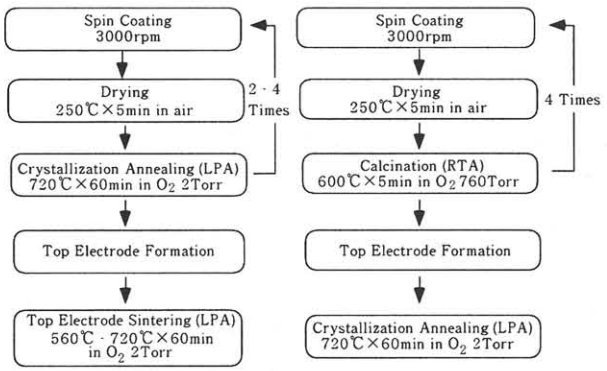

(a) Procedure-A (b) Procedure-B

Figure 1. Flow Charts of the MOD method by (a) Procedure-A, (b) Procedure-B.

Two MOD procedures were used for the preparation of SBT thin films. Figure 1(a) and (b) show these two procedures, i.e., Procedure-A and Procedure-B. In Procedure-A, low pressure annnealing (LPA) at 720℃ (susceptor temperature) was executed per coating. On the other hand, in Procedure-B, LPA was executed after all the layers were coated. The thickness of SBT film obtained in one coating was about 50 nm. For both procedures, a platinum top electrode with thickness of 100 nm was deposited on the SBT film by sputtering method, and the electrode was etched to the size of $2.56\times10^{-4}cm^2$.

Remanent porarization (Pr) and Ec of SBT films were measured using RT6000 (Radiant Technologies, Inc.). Leakage current density (I_L) was measured using 4145B (Yokogawa Hewlett Packard, Inc.). Surface morphologies and cross-sectional structures of the films were investigated by scanning electron microscopy (SEM).

3. Results and Discussion

Surface Morphology and Cross-Sectional Structure

Figure 2 and 3 show the surface morphologies and the cross-sectional structures of 200 nm-thick SBT thin films (4 layers) prepared by Procedure-A and Procedure-B. The SBT thin film prepared by Procedure-A exhibits dense structure with small grain size of 30 nm - 50 nm, whereas SBT thin film prepared by Procedure-B exhibits porous structure with large grain size of 100 nm - 200 nm.

The small grain growth and dense structure in case of Procedure-A are considered to be due to suppression of large grain growth for crystallization of 50 nm - thick thin film.

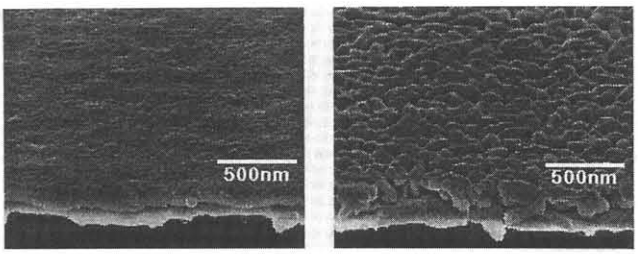

(a) Procedure-A (b) Procedure-B

Figure 2. Surface Morphologies of SBT films prepared by (a) Procedure-A, (b) Procedure-B.

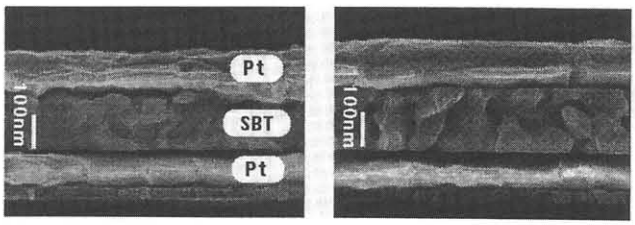

(a) Procedure-A (b) Procedure-B

Figure 3. Cross-Sectional Structures of SBT films prepared by (a) Procedure-A, (b) Procedure-B.

Electrical Properties

Figure 4 shows the P-E hysteresis loops of the 200 nm - thick SBT film prepared by Procedure-A, which exhibits well saturated properties above 100kV/cm. The ferroelectric characterisitics of the film are Pr=4.87 μ C/cm², Ec=23.8kV/cm, and $I_L=8\times10^{-8}A/cm^2$

at an applied field of 150kV/cm.

The I-V characteristics of the SBT thin films prepared by Procedure-A and Procedure-B are compared in figure 5. The breakdown voltage (V_B) of the film prepared by Procedure-B is about 7.6V, which is considered to be due to the porous structure. On the other hand, in the case of Procedure-A, V_B is over 20V, which is considered to be due to dense structure. Furthermore, even the 100 nm - thick film (2 layers) exibits V_B of about 10V, which means that the Procedure-A is effective for lowering the thickness of SBT films.

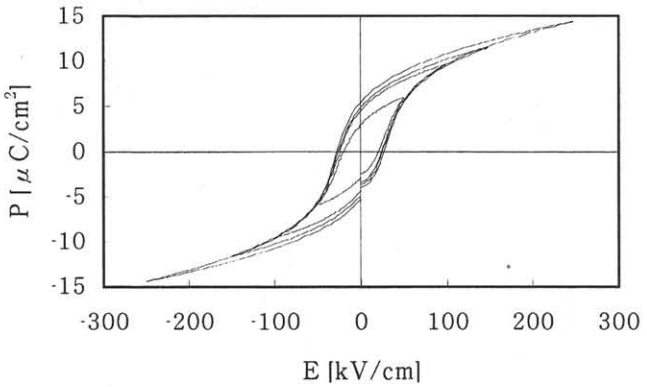

Figure 4. P-E hysteresis loops measured at various electric fields (50 - 250 kV/cm) of SBT films prepared by Procedure-A.

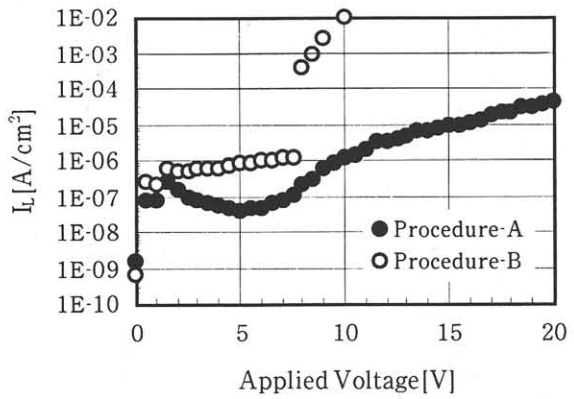

Figure 5. I-V characteristics of SBT films prepared by (a) Procedure-A, (b) Procedure-B.

Top Electrode Sintering

Figure 6 and 7 show Pr and I_L of 200 nm-thick SBT films at an applied field of 150kV/cm as a function of sintering temperature after the top Pt electrode deposition and etching. The Pr monotonically increases from 560 ℃ to 720 ℃, which means a progress of crystallization of the film. However, I_L is constant from 560℃ to 720℃. Futhermore, within this temperature range, V_B of all films are over 20V. Usually, the SBT films need high temperature sintering after the top Pt electrode deposition to suppress leakage current. But a film prepared by Procedure-A does not need high temperature sintering. It is considered that the film with dense structure sufficiently suppresses leakage current even without the top electrode sintering.

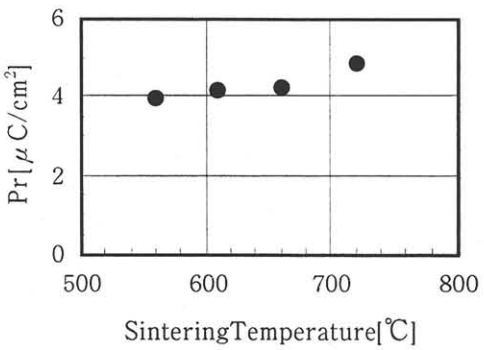

Figure 6. Pr of SBT films prepared by Procedure-A at various top electrode sintering temperatures.

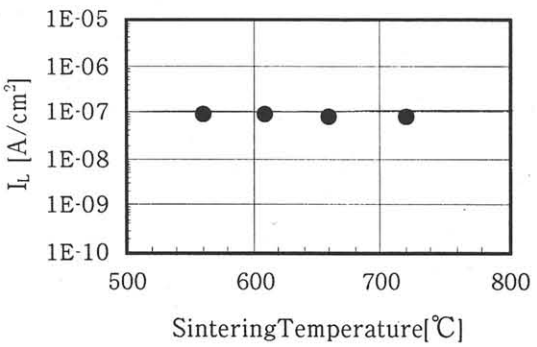

Figure 7. Leakage Current Density of SBT films prepared by Procedure-A at various top electrode sintering temperatures.

4. Conclusion

We proposed a new low pressure and low temperature processing method for MOD SBT thin films. The SBT thin films prepared by this method exhibited fine-grained and dense structure with grain size of 30 nm - 50 nm. The breakdown voltage of over 20V were obtained for the 200 nm-thick films annealed at 720℃ for 60 min in a 2Torr oxgen ambient per coating.

Acknowledgement

The authors would like to thank Mr. Y. Kawabata for his support and encouragement.

References

1) R. D. Nasby, J. R. Schwank, M. S. Rodgers, and S. L. Miller: *Proc. 3rd Int. Symp. Integrated Ferroelectrics* (1991) p. 376.
2) T. Mihara, H. Watanabe and C. A. Paz de Araujo: Jpn. J. Appl. Phys. **33** (1994) 3996.
3) C. A. Paz de Araujo, J. D. Cuchiaro, L. D. McMillan, M. C. Scott and J. F. Scott: Nature **374** (1995) 627.
4) T. Mihara, H. Watanabe, C. A. Paz de Araujo, J. Cuchiaro, M. Scott and M. D. McMillan: *Proc. 4th Int. Symp. Integrated Ferroelectrics* (1992) p. 137.
5) T. Li, Y. Zhu, S. B. Desu, C. H. Peng and M. Nagata: Appl. Phys. Lett. **68** (1996) 616.
6) Y. Ito, M. Ushikubo, S. Yokoyama, H. Matsunaga, T. Atsuki, T. Yonezawa and K. Ogi: Jpn. J. Appl. Phys. **35** (1996) 4925.